Dynamic Sand Dunes

Y. Amarouchene, J. F. Boudet, and H. Kellay
Centre de Physique Moléculaire Optique et Hertzienne (U.M.R. 5798), U. Bordeaux I, 351 cours de la Libération, 33405 Talence, France
(Received 10 July 2000; revised manuscript received 25 October 2000)

When sand falling in the spacing between two plates goes past an obstacle, a dynamic dune with a parabolic shape and an inner triangular region of nonflowing or slowly creeping sand forms. The angle of the triangular zone increases with the height of the dune and saturates at a value determined by the geometry of the cell. The width of the dune, related to the radius of curvature at the tip, shows universal features versus its height rescaled by geometrical parameters. The velocity profile in the flowing part is determined and found to be nonlinear. The parabolic shape can be accounted for using a simple driven convection-diffusion equation for the interface.

DOI: 10.1103/PhysRevLett.86.4286 PACS numbers: 45.70.Mg, 45.70.Ht, 45.70.Qj

Granular materials can exhibit very diverse features. This particular state of matter has so far resisted a coherent and quantitative description. Several experiments and theoretical attempts have been carried out [1]. A particular problem or subset of problems in the physics of granular materials is the different pattern formations observed when these materials are subjected to external perturbations such as shaking the container. Patterns, such as rolls similar to the ones seen when a fluid is heated from below, have been evidenced [2]. Such features encourage a continuum description, but other features such as the formation of arches [1] point to the importance of discreteness of the material. Our contribution here is in this spirit and asks the question of what happens when sand flows past obstacles. This experiment resembles flow past cylinders say in fluid mechanics. Such a flow configuration is well known by now and beautiful photographs of the different structures which form behind the cylinder can be found in the literature. When a granular material is used, two streams of dense material with no particular structure form behind the obstacle. The two streams are separated by an empty region due to the shielding by the obstacle (Fig. 1). Such a behavior is very different from the vortex shedding known in fluid dynamics. In the case of a granular material, the interesting behavior actually occurs on top of the obstacle where a dynamic dune with a parabolic tip forms (Fig. 1). Inside this parabola, a triangular region of nonflowing or slowly creeping sand is observed. The sand flow in the region between the triangular region and the outer parabola displays a velocity profile which is nonlinear. The coexistence of both still or very slowly creeping and flowing regions clearly shows the complexity of sand flow in a simple situation. Here we present a study of the properties of this dynamic dune as well as an attempt to describe it using models available in the literature [3–5]. Our study points to the possibility of describing such patterns using a convection-diffusion equation. This experiment is a simple test ground for interface dynamics of granular materials, their flow properties as well as the complicated process of dune formation.

In our experiments, the flow of sand is maintained between two parallel transparent plates (Plexiglass or glass) with a fixed spacing e which we varied from about 2 to 8 mm. An obstacle is then blocked between the plates. Dry beach sand (which has been sieved to eliminate large particles and washed to eliminate the smallest particles) is

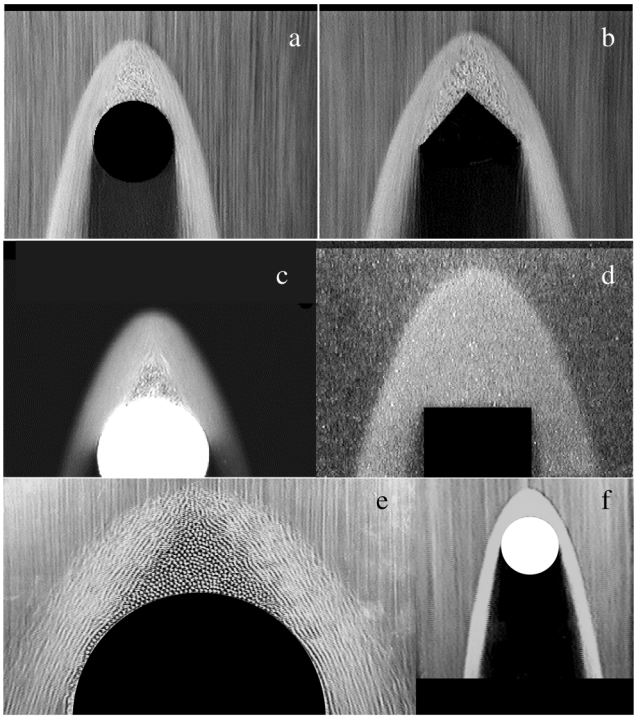

FIG. 1. Photographs of patterns formed by flowing sand around obstacles: circle [$R = 1.2$ cm (a), $R = 1.4$ cm (c)]; triangle (base of 3 cm) (b) (dry beach sand, exposure time $1/50$ s); flat obstacle (length of 2.4 cm) (d) (glass beads, exposure time of 10^{-4} s). Glass plates are used for (a) and (b) and Plexiglass plates for (c) and (d). Note in photo (c) the triangular inner region with little motion blur. (e) Ball bearings of diameter 2 mm ($e = 6.2$ mm and $R = 6$ cm); (f) glass beads ($R = 2.25$ cm, $e = 6.2$ mm) showing the full view including the wake in the form of two streams.

 0031-9007/01/86(19)/4286(4)$15.00

poured in the spacing between the plates from a wedge-like container, the bottom of which has an opening in the shape of a long rectangle with variable width and a fixed length L much larger than the size of the obstacle. The sand which falls between the two plates undergoes free fall. As a grain hits the solid obstacle, it bounces back with a parabolic trajectory. When the number of grains hitting the obstacle increases (which we do by changing the mass flux through changing the width of the opening of the upper container), a few particles get trapped on top of the obstacle. This arrest of the movement of particles becomes more and more important as the flux of particles increases. From a few grains on top of the cylinder, a large triangular region of nonflowing or slowly creeping sand can be formed at high injection rates. While we are still investigating the details of formation of the dune, an interesting possibility here is that the arrest of the particles on top of the obstacle resembles the clumping or "inelastic collapse" seen in simulations of one-dimensional granular systems [6]. This clumping clearly shows that hydrodynamic descriptions are difficult to implement in the flow of granular materials. Recent experiments [7] and numerical simulations [8] give evidence of such a collapse in two and three dimensions. In our experiments a similar behavior is observed pointing to the complexity of such flows. On the one hand, a rapidly flowing region is present; on the other hand, a triangular cold clump occupies the center of the pattern. Let us note here that these experimental observations are robust with respect to the granular materials used, such as glass beads, ball bearings, and nonsieved dry beach sand which is much more polydisperse and with respect to the material of the plates which was either glass or Plexiglass. While the distance between the obstacle and the entrance was kept constant for most of the experiments reported here we did note that the height of the dune decreases slightly when the obstacle is placed much farther away.

The photos in Fig. 1 show the shape of the sand dunes around a circular obstacle (a), a triangular obstacle (b), and a flat obstacle (d): the main features seem to depend little on the geometry of the obstacle itself. The photos in Figs. 1(a) and 1(b) (using sieved dry beach sand, mean diameter: 0.3 mm) clearly display two regions: an inner region with little motion blur indicating small velocities and a blurred region where the velocity can reach several cm/s. Figure 1(d), for which we use glass beads (mean diameter of 0.5 mm), is taken using an exposure time of 10^{-4} s to illustrate the small roughness of the interface. For Fig. 1(c), which was taken in transmission, several photos were averaged to illustrate the two different regions more clearly. The inner still or slowly creeping region is triangular as can be seen in 1(c); the blurry region contains flowing sand. Figure 1(e) shows a dune formed using ball bearings of 2 mm diameter to illustrate the insensitivity of the observed shape with respect to the material used. Figure 1(f) shows a wide view of the whole structure including the wake behind the obstacle consisting of simply two streams of structureless dense material. The overall shape of the pattern is parabolic as illustrated by the solid line in Fig. 2 for a circular obstacle. The interface shape is given by $h(x) = H - \frac{x^2}{2R_c}$ where H is its height as counted from the top of the obstacle and R_c the radius of curvature at the tip of the parabola. The sand is flowing slowly near the triangular region and much faster near the outer edge. In the region delimited by the outer parabola and the triangular still inner region, a velocity profile is established. This figure contains examples of the trajectories of two particles in the flowing region which were determined from directly tracking the particles using a fast video camera with a rate of 250 images per second giving a time step of 4 ms. The particle trajectories are roughly straight lines with the velocity almost constant along such lines. The small fluctuations seen are within experimental uncertainty in determining the position of the particles. These trajectories are also roughly parallel to each other and roughly parallel to the line delimiting the static zone. The total velocity increases dramatically as the outer region is approached starting from the inner triangular region. From tracking several particles in the flowing region, a velocity profile is determined. A cut of this velocity profile perpendicular to the trajectories of the particles and to the line delimiting the inner zone is displayed in Fig. 3. This profile is nonlinear and increases from very small velocities near the inner triangular region to very large velocities near the outer parabola. This velocity profile is plotted against a reduced distance $(\frac{d}{d_0} - 1)$ for different realizations with different dunes and different grain types. Here d is the distance from the top of the obstacle along a cut perpendicular to the line delimiting the inner triangular region and d_0 is the position of the intersection point (see Fig. 2). The data show too much scatter for a critical test of theoretical predictions [9]. Our results seem to be consistent with recent experiments where the mean velocity of the layer of sand was found to increase as its height increases [10,11]. Within the triangular region, we found it very difficult to measure the movement of the particles as they hardly moved during the time scale of the experiments which could last as long as

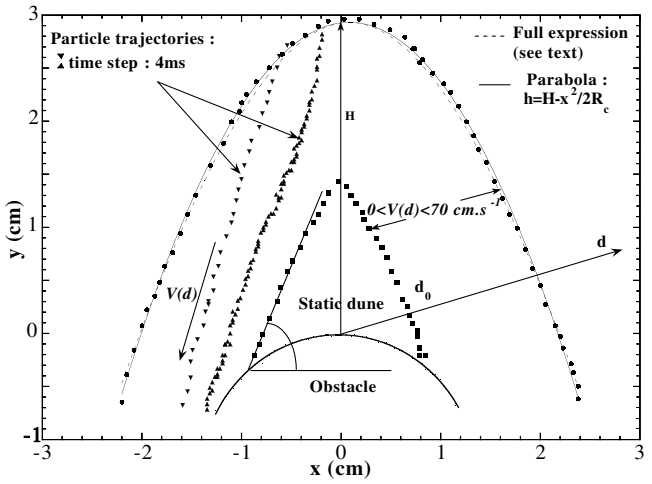

FIG. 2. Anatomy of the dune.

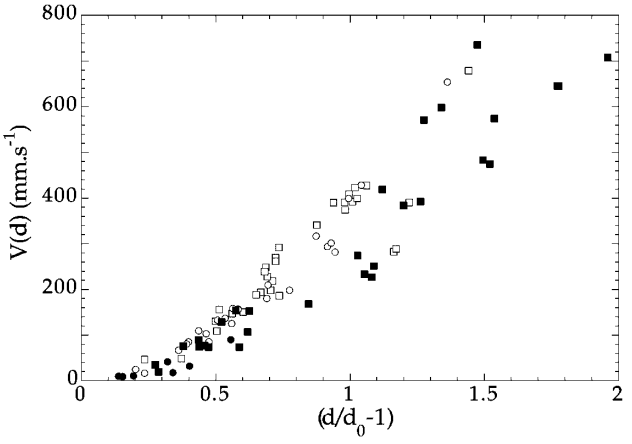

FIG. 3. Velocity profile in the dune versus $(d/d_0 - 1)$ (see Fig. 2) obtained by tracking several marked particles in the flowing region of the dune.

10 s which gives an upper bound for the velocity in this zone of much less than 1 mm/s. Our observations do not rule out the possibility of creep flow in this region especially near d_0 [12].

To quantify these patterns, measurements of the height of the parabola H, the radius of curvature R_c, and the angles of repose θ of the inner triangular region are carried out for different circular obstacles. The mass flux of particles Q (mass per unit time) of sand as well as the spacing between the plates e and the radius of the obstacle R were varied. Q values ranged from 0.5 to 0.05 kg/s, R values changed from 5 to 30 mm, and e changed from 1.8 to 8 mm (the ratio e to grain size ranged from about 6 to about 25 for sand grains). The idea here is to test whether the patterns observed are independent of geometrical parameters. We find that H increases linearly versus the mass flux of grains Q; also, for a fixed flux this height turns out to be linearly proportional to the radius of the circular obstacles and inversely proportional to the square of the spacing between the plates: $H \sim QR/e^2$ as can be seen in the inset of Fig. 4.

The dependence of R_c/R versus H alone turns out to be quite complicated. We noted, for example, that R_c/R starts close to 1 and decreases to smaller values as H increases; however we also observed that R_c/R goes through a minimum and increases as H becomes very large. Despite this complicated behavior we did find a way to rescale our data in a simple fashion by using He/R which is simply proportional to the mass flux Q per unit area (Le) and $\sqrt{2R_cH}$, the half-width of the parabola at the level of the top of the obstacle. Figure 4 shows the variation of $[(\sqrt{2R_cH})/R]$ versus $\frac{He}{R^2}$ found using different diameter circles, different spacings e, different flow rates, and different grain types; the data from different realizations fall on straight lines for almost the whole range of values of He/R^2 except at small values of this parameter where a steep decrease is observed.

A distinguishing feature of the inner triangular region is its high angle of repose which can reach values as

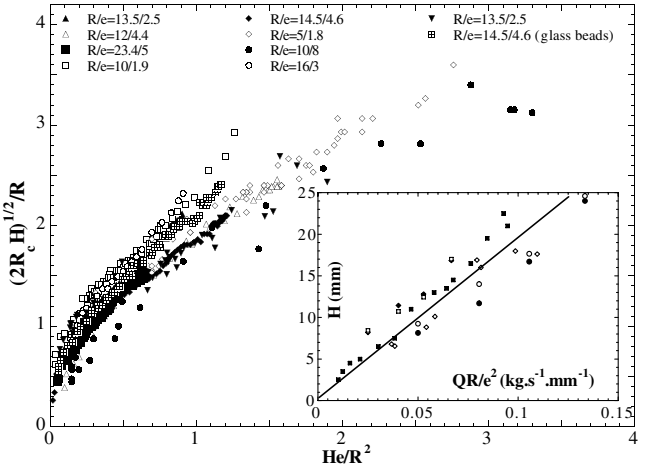

FIG. 4. The variation of $[(\sqrt{2RcH})/R]$ versus He/R^2. Inset: H versus QR/e^2 (kg/s mm). Filled squares: Q varies while R and e are constant; diamonds: e varies with R and Q/e being constant. The rest of the symbols are for a constant e but with Q and R being variable.

high as 80°. Figure 5 shows the angle of repose θ of the inner zone as a function of the height of the dune H. The higher the dune the higher is the angle of repose. These measurements are done for different diameters of the obstacle, varying particle mass flux, and different spacings e. Note that above a certain height the angle seems to saturate at a certain value $\theta_{\max}$ determined directly by the ratio R/e as indicated by the horizontal lines $[\tan(\theta_{\max}) = R/e]$. The flowing sand must exert extra pressure on the inner pile for it to have a large angle of repose. Clearly a question to be addressed is the relation between the flow characteristics and the angle of repose, a difficult issue at the present time [13]. The simple law for the variation of the maximum angle with the ratio R/e points however to geometrical reasons for the stability of such high angles; since $\tan(\theta)$

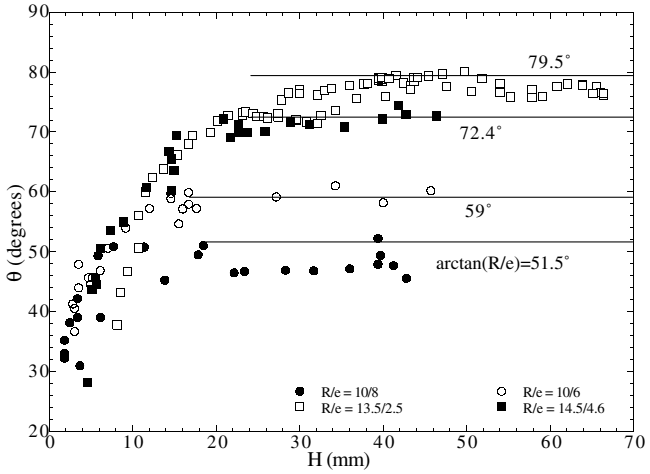

FIG. 5. Angle of repose of the triangular region as a function of the height of the dune for various R/e. The dimensions are given in millimeters. Note the saturation at $\tan(\theta_{\max}) = R/e$ as indicated by the horizontal lines.

measures a friction coefficient, our result indicates that this coefficient depends first on the height of the dune and saturates at a value fixed by the geometry. We have made other interesting observations: the height of the triangular region as well as $\tan(\theta)$ increases linearly versus H at first but then saturates at larger values of H; this is the point where the angle starts to saturate. For these large values of H only the flowing region continues to grow as H increases. Incidentally, this is also the point where the radius of curvature of the parabola goes through a minimum.

Before we conclude, let us mention that the use of a simple phenomenological model for the interface of the pattern leads to shapes which are very close to the shapes seen in this experiment. This model is borrowed from recent theoretical attempts to understand avalanche dynamics [3–5]. In a sense, the interface height is postulated to obey a convection diffusion equation as for say a dye concentration convected by a velocity field. This can be written as $\partial_t h - v\partial_x h = D\partial_{xx} h + q$. The left-hand side expresses the convection of the interface height h by a constant velocity v parallel to the horizontal axis x. The right-hand term includes a characteristic constant vertical velocity q acting as a source term and a diffusive term with a diffusion constant D. The presence of the diffusive term may be related to the roughness of the patterns as evidenced by taking photographs with a fast shutter speed. A solution of this equation in the stationary case gives the following interface height profile: $h(x) = H - q/v\, x + Dq/v^2[1 - \exp(-vx/D)]$. H is simply the height of the dune at its center. A direct fit to the profile gives very good agreement with experiments as seen in Fig. 2 (the values of the parameters extracted from the best fits are q/v between 4 and 6, D/v between 2.24 and 3.78 cm, and D/q between 0.56 and 0.63 cm, to be compared to the value of R_c of 0.75 cm extracted from the parabolic fit). The value of q turns out to be close to a typical vertical velocity extracted from the variation of H versus Qe/R^2 which is about 100 cm/s (a typical value of v is about 20 cm/s). The value of D turns out to be about 60 cm^2/s. If one sets $D = V\zeta$ where V is a typical velocity parallel to the interface and ζ a typical diffusion length, the numbers above would give a diffusion length less than a centimeter. In fact, the calculated profile is very close to the parabolic shape in case the term vx/D is small. Since V is much larger than v as we checked experimentally, the approximation can be justified. An expansion of the exponential factor can be carried out and what remains is just H and the second order term. In this limit one can write $h(x) = H - q/Dx^2$. This form gives an expression for the radius of curvature of the parabola as $R_c = D/q$. This expression can be used in conjunction with our experimental findings to give the variation of D/q versus flow properties. In any case, and in the limit of validity of this model, the measurement of R_c is a direct measure of D/q. Let us mention that if we do not include a diffusive term, we would find linear profiles. Our experiment points to the possible relevance of diffusive transport for interface dynamics in granular flows as has been argued theoretically. Despite this encouraging simplicity, the presence of an inner nonflowing or slowly creeping zone with some curious features such as its high angle of repose determined by geometry leaves some unanswered questions.

We studied pattern formation in a novel situation: the flow of a granular material around obstacles in a quasi-two-dimensional situation. The patterns observed which are dynamic sand dunes form on top of the obstacle, have parabolic shapes, and present an inner triangular region where the sand is nonflowing or slowly creeping. The flow between this inner part and the outer parabola displays a nonlinear velocity profile. The radius of curvature at the tip and the angle of repose display intriguing behavior and some universality. A simple model based on a convection diffusion equation for the interface of the dune seems to account for the parabolic shapes observed.

We thank O. Greffier, B. Andreotti, A. Würger, J. Meunier, B. Bonnier, and Y. Leroyer for discussions, and T. Douar for help with the experiments.

[1] S. R. Nagel, Rev. Mod. Phys. **64**, 321 (1992); M. Jaeger, S. R. Nagel, and R. P. Behringer, Rev. Mod. Phys. **68**, 1259 (1996); J. Duran, *Sables, Poudres et Grains* (Eyrolles Sciences, Paris, 1997); P-G. de Gennes, Rev. Mod. Phys. **71**, 374 (1999); L. P. Kadanoff, Rev. Mod. Phys. **71**, 435 (1999).

[2] F. Melo, P. B. Umbanhowar, and H. L. Swinney, Phys. Rev. Lett. **75**, 3838 (1995); P. B. Umbanhowar, F. Melo, and H. L. Swinney, Nature (London) **382**, 793 (1996); J. R. de Bruyn *et al.,* Phys. Rev. Lett. **81**, 1421 (1998).

[3] J.-P. Bouchaud *et al.,* J. Phys. I (France) **4**, 1383 (1994); J.-P. Bouchaud *et al.,* Phys. Rev. Lett. **74**, 1982 (1995).

[4] T. Boutreux, E. Raphael, and P-G. de Gennes, Phys. Rev. E **58**, 4692 (1998); A. Aradian, E. Raphael, and P-G. de Gennes, Phys. Rev. E **60**, 2009 (1999).

[5] L. Mahadevan and Y. Pomeau, Europhys. Lett. **46**, 595 (1999).

[6] Y. Du, H. Li and L. P. Kadanoff, Phys. Rev. Lett. **74**, 1268 (1995).

[7] A. Kudrolli, M. Wolpert, and J. P. Gollub, Phys. Rev. Lett. **78**, 1383 (1997).

[8] I. Goldhirsch and G. Zanetti, Phys. Rev. Lett. **70**, 1619 (1993); S. McNamara and W. R. Young, Phys. Rev. E **50**, R28 (1994); S. Chen *et al.,* cond-mat/9804235.

[9] R. A. Bagnold, Proc. R. Soc. London **225**, 49 (1954).

[10] O. Pouliquen, Phys. Fluids **11**, 542 (1999).

[11] E. Azanza, F. Chevoir, and P. Moucheront, J. Fluid. Mech. **400**, 199 (1999).

[12] T. Komatsu *et al.,* cond-mat/0008086.

[13] S. Douady, B. Andreotti, and A. Daerr, Eur. Phys. J. B **11**, 131 (1999).